CONCRETE LIBRARY OF JSCE NO. 23, JUNE 1994

APPLICATION OF MULTI-PHASE MODEL TO THE PIPE FLOW OF FRESH CONCRETE

(Reprinted from Proc. of JSCE, No.466, V-19, 1993)

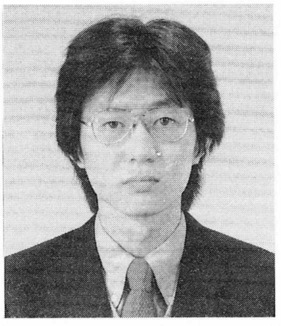
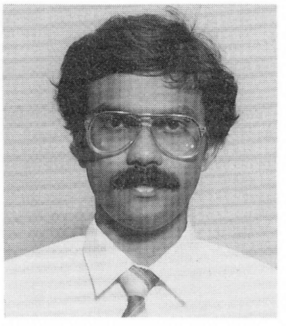
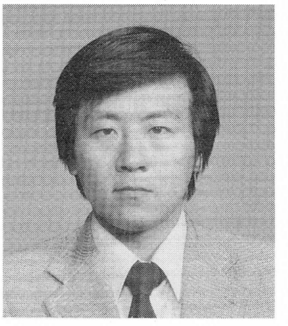

Kazumasa OZAWA   Anura S.M.NANAYAKKARA   Koichi MAEKAWA

SYNOPSIS

This paper proposes a mechanical model in terms of the collisional and frictional interaction of constituent particles for the flow of fresh concrete through pipelines. The multi-phase formulation was adopted as the basis for computing resistance to the deformation arising in tapered and bent pipes. The effect of cement paste existing in fresh concrete on the particle interaction of sands and gravels was taken into account. Approximately 20 different mixtures of concrete were examined for verification of the numerical modeling. The analytical model was proved to be enough to handle a wide variety of fresh concrete having 3-27 cm by slump and any type of deformed pipe unit with different dimensions. It emphasized that the pump pressure of concrete being driven through the deformed pipe units can be predicted well by the particle interaction model of aggregates and the multi-phase scheme.

Keywords: multi-phase flow, pumpability, fresh concrete, pipeline, deformability

K.OZAWA is an associate professor of Department of Civil Engineering, the University of Tokyo, Japan. He obtained his Dr.Eng. from the University of Tokyo in 1991. His research interest covers self-compactable high performance concrete, mechanical behavior of fresh concrete and construction system for concrete structures.

A.S.M.NANAYAKKARA is a lecturer of Department of Civil Engineering, University of Moratuwa, Sri Lanka. He obtained his Dr.Eng. from the University of Tokyo in 1990. He was a former graduate student of the University of Tokyo, Japan.

K.MAEKAWA is an associate professor of Engineering Research Institute, the University of Tokyo, Japan. He obtained his Dr.Eng. from the University of Tokyo in 1985. His research interests covers reinforced concrete mechanics, computational approach to seismic behaviors of RC-Soil system, thermodynamics of cement-concrete composite, and durability design of concrete structures.

1. INTRODUCTION

The recent demand for high-grade fresh concrete presents an ungent engineering matter in the form of rationalization of concrete construction, especially under the present social background of Japan[1]. A unified approach to the mechanics of fresh concrete is needed to make versatile material design and development possible. High performance concrete[2], which is self-compactable despite complex arrangements of reinforcement and is also highly durable at the hardened stage, is regarded as one of targets of the advisable mechanics concerned.

The authors have sought a multi-phase model for the pipe flow of fresh concrete and examined what type of behavior the numerical approach could qualitatively cover as regards the deformation of fresh concrete in shear produced in tapered and bent pipe units[3]. Here, the concept of partial stress is newly introduced. This paper aims at proposing material constitutive models to represent the particle-to-particle interaction of gravel, sand, and cement paste.

In establishing the relation of stress versus strain rate for concrete components, we focused on the pressure drop which is necessary to sustain a stable particulate flow through deformed pipe units. The flow rate and associated total pressure were measured around those boundary conditions of various dimensions with systematically arranged mixtures of fresh concrete[3].

In this study, deformed pipe units are regarded as the testing apparatus the specified mode and intensity of particle-to-particle interaction is reproduced[6]. The measured pressure is the resultant force due mainly to particle interactions and the reaction from the pipe wall. It can be said that the relationship between pressure measured at the inlet of the pipe and the corresponding strain rate,which has been formulated with respect to the rate of flow[4,5], exhibits the stiffness of the particulate flow.

Pump transportation technology of fresh concrete plays an indispensable role in model construction work to its greater efficency. Integration of the pump construcction method with recent high performance concretes will be realizable in the near future. Hence, it is expected that a multi-phase model for fresh concrete flow and material constitutive models will result in a mixture design procedure based on the requirements for fluidity, consistency and pumpability. Approximately 40 cases with a wide variety of mixtures and deformed pipe dimensions were examined for verification of the proposed multi-phase formulation and the particle interaction models of components in concrete.

2. GOVERNING EQUATION

The authors have proposed a general formulation for multi-component solid a nd liquid phases and verified its performance[3]. Since details have already been reported and cannot be covered within the limited space available here, this chapter summarizes the framework of system formulation. In the proposed scheme for multi-phase formulation, the sectional averaged volume fractions of gravel, sand, powder, and water are defined as Cg, Cs, Cp and Cw. The volume fractions vary in both time and space domains under the requirement of mass conservation described by,

$$\frac{\partial(AC_i \cdot u_i)}{\partial s} + A\frac{\partial C_i}{\partial t} = 0 \cdots\cdots\cdots\cdots (1)$$

where, u_i is the sectional averaged rate of flow of the assembly of phase " i" , and the notation " A " indicates the cross sectional area defined along the axial coordinate denoted by " s " , as shown in Fig.1.

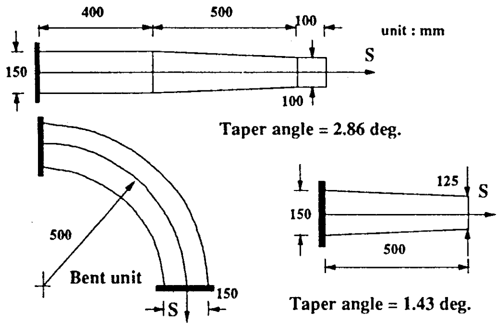

Fig.1 Analysis target and the coordinate.

Regarding four phase system, we must satisfy the following requirement of volume compatibility.

$$C_g+C_s+C_p+C_w=1 \qquad (2)$$

For focusing on the segregation of gravel and mortar, we can degenerate the degrees of freedom with respect to the speed of the phases as,

$$\left.\begin{array}{l} u_w=u_p=u_s\,(\equiv u_m) \\ u_g\neq u_m \end{array}\right\} \qquad (3)$$

A further requirement of the mechanical dynamics is the conservation of momentum of each phase. Reduction of the degrees of freedom yields,

$$-\frac{\partial(A\sigma_g)}{\partial s}-2\pi R\tau_g+S_{mg}+\rho_g C_g g_s A$$
$$=\rho_g C_g A\left(\frac{\partial u_g}{\partial t}+u_g\frac{\partial u_g}{\partial s}\right) \qquad (4)$$

$$-\frac{\partial\{A(\sigma_s+\sigma_p+\sigma_w)\}}{\partial s}-2\pi R(\tau_s+\tau_p+\tau_w)$$
$$-S_{mg}+(\rho_s C_s+\rho_p C_p+\rho_w C_w)g_s A$$
$$=(\rho_s C_s+\rho_p C_p+\rho_w C_w)A\left(\frac{\partial u_m}{\partial t}+u_m\frac{\partial u_m}{\partial s}\right)$$
$$\qquad (5)$$

where, σ_i and τ_i are defined in the i-phase as the sectional averaged partial normal stress and the peripherally averaged partial shear stress developed at the pipe wall. The value of Smg represents the drag force associated with the segregation of the gravel and mortar phases. ρ_i is the net density of particles in the i-phase and g_s is the gravity acceleration in the direction of the s-axis.

The partial stresses of each phase comprise the contact stresses generated by particle-to-particle interaction in the individual phase concerned and by the stresses applied on the coarser components by the other phases with finer particles. Namely,

$$\left.\begin{array}{l} \sigma_w=(1-C_g-C_s-C_p)\cdot P \\ \tau_w=(1-C_g-C_s-C_p)\cdot\tau_{cw} \end{array}\right\} \qquad (6\text{-}1)$$

$$\left.\begin{array}{l} \sigma_p=(1-C_g-C_s)\cdot\sigma_{cp}+C_p\cdot P \\ \tau_p=(1-C_g-C_s)\cdot\tau_{cp}+C_p\cdot\tau_{cw} \end{array}\right\} \qquad (6\text{-}2)$$

$$\left.\begin{aligned}\sigma_s&=(1-C_g)\cdot\sigma_{cs}+C_s\cdot(\sigma_{cp}+P)\\ \tau_s&=(1-C_g)\cdot\tau_{cs}+C_s\cdot(\tau_{cp}+\tau_{cw})\end{aligned}\right\}\cdots\cdots\cdots(6\text{-}3)$$

$$\left.\begin{aligned}\sigma_g&=\sigma_{cg}+C_g\cdot(\sigma_{cs}+\sigma_{cp}+P)\\ \tau_g&=\tau_{cg}+C_g\cdot(\tau_{cs}+\tau_{cp}+\tau_{cw})\end{aligned}\right\}\cdots\cdots\cdots(6\text{-}4)$$

where, σ_{ci} and τ_{ci} are the contact stresses in sectional averaged compression and shear. The parameter P is defined as the pore liquid pressure and is equal to σ_{cw}. The contact stress of each phase can be predicted by the constitutive laws, provided that the local strain rate is derived from the field of flow. The authors described the flow field and deformation of dense solid-liquid indicated by,

$$J_g=0 \qquad \text{for a straight pipe} \cdots\cdots(7\text{-}1)$$

$$J_g=\frac{\sqrt{3}}{R}\cdot\tan\theta\cdot u_g \qquad \text{for a tapered pipe} \cdots\cdots(7\text{-}2)$$

$$J_g=\frac{\phi}{2}\cdot u_g \qquad \text{for a bent pipe} \cdots\cdots(7\text{-}3)$$

$$\left.\begin{aligned}J_s&=\left(\frac{1}{1-C_g}\right)\cdot J_g\\ J_p&=\left(\frac{1}{1-C_g-C_s}\right)\cdot J_g\end{aligned}\right\}\cdots\cdots\cdots(8)$$

where, J_i indicates the sectional averaged second invariant of strain rate of each phase in the fresh concrete[4,5,7].

The values of R, θ , and ϕ indicate the dimensions of deformed pipes; that is, the radius of the section, the taper angle, and the curvature of the bent pipe. This invariant represents the intensity of the shear mode rate of deformation of the particle assembly.

According to experiments with various taper angles under low rates of flow, direct proportionality was reported regarding the shear rate[4] and the particle interaction stress[6]. Then we have,

$$\left.\begin{aligned}\sigma_{cg}&=K_g\cdot J_g\\ \sigma_{cs}&=K_s\cdot J_s\\ \sigma_{cp}&=K_p\cdot J_p\\ K_p&=0\end{aligned}\right\}\cdots\cdots\cdots(9)$$

$$\left.\begin{aligned}\tau_{ci}&=\left(\frac{\mu_i+\theta}{1-\mu_i\cdot\theta}\right)\cdot(\kappa_i\cdot\sigma_{ci}+\theta\cdot\tau_{vi})+\tau_{vi}\\ \tau_{vi}&=\tau_{v0,i}+\eta_i\cdot u_i\end{aligned}\right\}\cdots\cdots(10)$$

where, K_i is the axial stiffness of each phase and κ_i represents the lateral stress ratio as one of the constitutive laws. The value of τ_{vi} is the viscous shear stress composed of the yield stress denoted by $\tau_{v0,i}$ and the viscosity coefficient, η_i .

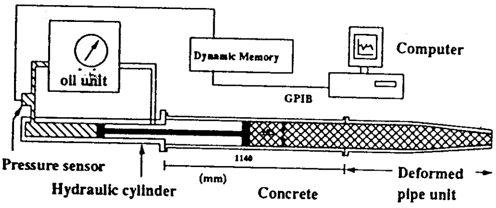

Fig.2 Experimental set-up for pumping resistance test[6].

The segregation resistance is involved as the phase interaction force. Experiments on the drag force applied to spherical balls yielded the following formulation[3,13]:

$$\left.\begin{aligned} S_{mg} &= \left(\frac{3AC_g}{4\pi a^3}\right) D_s \\ D_s &= H\cdot a\cdot (u_m - u_g) + a^2 T \end{aligned}\right\} \cdots\cdots\cdots\cdots\cdots\cdots (11)$$

where the mean diameter of particles is defined as " a " and the values of H and T are viscosity parameters representing features of the drag force as applied to the particles.

3. MATERIAL MODELS OF FRESH CONCRETE

The pressure needed to sustain a stable flow of fresh concrete around a deformed pipe was measured with the variety of mix proportions and pipe dimensioms[6]. Since the table pressure obtained can serve to establish the particle interaction model through the multi-phase approach, the authors adopted the experimental cases where segregation and associated instability[3] were not observed in terms of the measured pressure. Hence, the computed pressure mainly depends on the particle interaction models described by Eq.(9) and Eq.(10).

In fact,the yield force and the viscosity for segregation resistance in Eq. (11) were numerically verified and found not to influence the total pressure if great enough to avoid substantial segregation in analysis[3]. In this study, the segregation resistance model is not substantial but the interaction of particles is the main issue considered. Then, values of viscosity and yield force high enough to avoid segregation were used in computation, actually, T=3.5 gf/cm² and H=1.0kgf*s/cm².

(1) Model of Aggregates
As discussed in computational simulation[3], the pressure loss caused by the deformed pipe units primarily results from aggregate particle interactions. First, the authors focused on different aggregate mixtures with a common water-to-cement ratio by volume. The experiment to measure the pressure caused by the deformed pipes was conducted using the pumping resistance test apparatus shown in Fig.2[6].

Fig.3 and Fig.4 show the total pressure needed to produce a stable flow of concrete in the bent pipe[6]. The flow rate was approximately 5± 1 cm/s and water-to-cement ratio by volume was 112%. The parameters were specific volume fractions of gravel and sand as formulated by $Cg/Cg_{,lim}$ and $Cs/(1-Cg)/Cs_{,lim}$ where $Ci_{,lim}$ means the limit compact volume concentration of the i-phase. These parameters indicate how densely the aggregates are suspended in the matrix. It has been reported that the same pressure drop can be expected when the specific volume fraction is common no matter what the shape and grading of the aggregates[6].

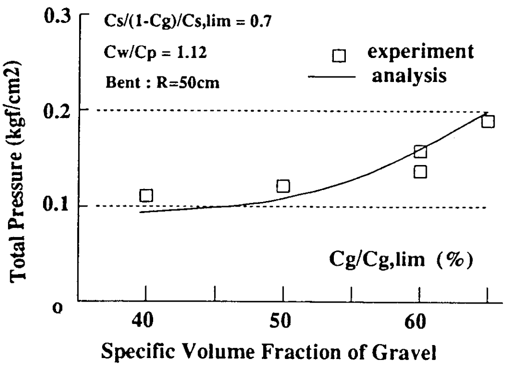

Fig.3 Total pressure at the inlet of bent pipe with respect to the mixture content of gravel.

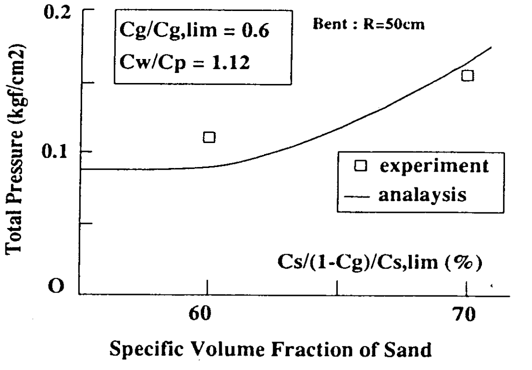

Fig.4 Total pressure at the inlet of bent pipe with respect to the mixture content of sand.

The authors assumed the stiffness Ks for one specific volume fraction of sand Cs/(1-Cg)/Cs, lim , for instance 70%, and next, inversely calculated the stiffness of the gravel phase in terms of the specific volume fraction as Cg/Cg , lim so that the pressure data for that particular volume coincide with the analytical results. Next, using the obtained stiffen of gravel, we checked the pressure data for different sand volume contents with a constant volume fraction of gravel. If good coincidence could not be found, the assumed stiffness of the sand was modified until all test results for the 112% water-to-cement ratio by volume are fairly predicted.

For analysis, the finite difference scheme[3] was adopted to seek for simultaneous solutions which satisfy the governing equations in section 2. The rate of flow and the volume fractions of each component at the inlet of pipe formed the boundary conditions. The analytical solutions in Fig.3 and Fig.4 were obtained for a 5 cm/sec constant flow rate at the inlet.

Finally the authors developed a stiffness model for aggregate particle assemblies based on the experiments with bent pipes as shown in Fig.5. This is formulated by the following equations:

$$K_g|_{\frac{C_w}{C_p}=1.12}=0.14\cdot\tan\left\{5.84\left(\frac{C_g}{C_{g,\lim}}-0.42\right)\right\}\geq 0 \quad \cdots\cdots (12)$$

$$K_s|_{\frac{C_w}{C_p}=1.12}= 0.274\cdot\tan\left\{0.58\left(\frac{C_s}{(1-C_g)C_{s,\lim}}-0.59\right)\right\}\geq 0 \quad \cdots\cdots (13)$$

Here, we assumed a frictional coefficient of 0.4 between aggregate and the pipe wall in Eq. (10) [8]. Since water is a non-frictional material whose friction against a solid is independent of the pore pressure, the frictional coefficient of water has to be zero.

The viscous drag stress for aggregates in Eq. (10) must be zero, but the water and powder mixture appears to have some cohesive viscosity. Tanigawa et al. carried out a one-plane direct shear test where the rate dependent and independent stresses were proved. As for the paste shear corresponding to a 112% water-to-cement ratio by volume, typical values were tentatively adopted according to Tanigawa et al.[9] as,

$$\left.\begin{array}{l}\tau_{v0,w}+\tau_{v0,p}=0.8\times 10^{-3}\ \mathrm{kgf/cm^2}\\ \eta_w+\eta_p=0.2\times 10^{-4}\ \mathrm{kgf\cdot s/cm^3}\end{array}\right\} \cdots\cdots (14)$$

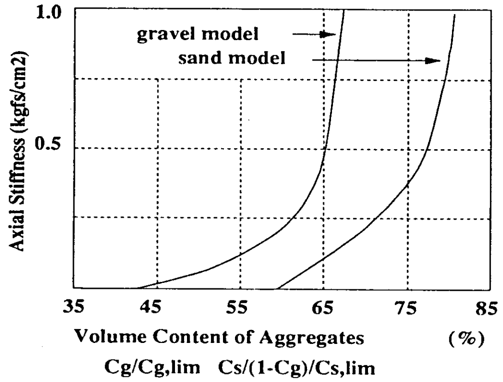

Fig.5 Assumed stiffness of aggregates with respect to the specific volume fraction of aggregates.

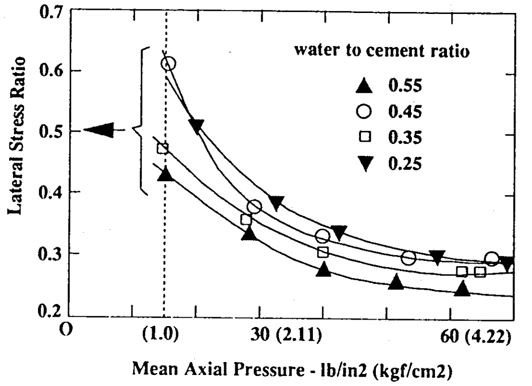

Fig.6 Variation of the lateral stress ratio of concrete with respect to the mixture and axial pressure[8].

It has been reported by Ede[8] that the lateral stress ratio of concrete obtained for a straight pipe varies according to the mixture as well as the mean axial pressure as shown in Fig.6. Since there is no lateral deformation along the axis of a bent pipe as in a straight one, it can be assumed that the lateral stress ratio in a concerning bent pipe is the same as that for a straight pipe. The value of the lateral stress ratio of concrete is approximately 0.5 around the pressure used in this series of experiments[6].

Since the stress of fresh concrete is carried by each component as idealized by Eq. (6), the lateral stress ratio is the resultant derived from Eq.(10), Eq. (6) and the specific mix proportion. Consequently, it cannot be theoretically concluded that the lateral stress ratio of concrete as shown in Fig.6 does not correspond to the lateral stress ratio of the aggregates. In fact, if we consider an extreme case where the concrete contains no solids particles(liquid phase only) , the lateral stress ratio must be unity and equal to κ_w because of its perfect isotropy.

However,it may be allowable to consider that the measured lateral stress ratio of concrete selected in Fig.6 will be close to the lateral stress ratio of the aggregates as constituent materials of concrete, because the total stress of concrete is carried by the aggregates in the case of ordinary mixture of fresh concrete (but not self-compactable concrete). Where lateral displacement is restricted, Tangtermsirikul related the local contact friction of the lateral stress factor using the micro contact theorem[10], showing that $\kappa=0.5$ corresponds to a friction coefficient of 0.33 at particle contact. The computation related in Fig.3 and Fig.4 was performed with a lateral stress ratio of 0.5 for aggregates regarding the deformation mode arising in bent pipe.

Fig.7 and Fig.8 show the pressure loss produced by the deformation of fresh concrete in tapered pipes[6]. It was clarified that the mode of deformation is pure shear in both tapered and bent pipes, but the direction of the principal axis of deformation in a tapered pipes is 45 ° away from that in a bent unit[4,5]. Since lateral deformation is agitated by the main axial flow in a tapered pipe, unlike a bent pipe, comparatively greater lateral stress will be obtained when the particles are packed so densely, because the particles cannot easily escape in the axial direction against the axial repulsion caused by particle collisions. This is not the case in bent pipes, where the principal direction of shear does not coincide with the axial direction of the main flow[5], and the lateral stress ratio is thought to have no relationship with the density of the aggregates. Accordingly, as regards the lateral stress ratio in tapered pipes, the authors tentatively propose the following model which depends on the specific volume fraction of gravel:

$$\left.\begin{array}{ll}\kappa_g=0.2 & \text{for } \dfrac{C_g}{C_{g,\lim}}\leq 0.5 \\ \kappa_g=6\dfrac{C_g}{C_{g,\lim}}-2.8 & \text{for } \dfrac{C_g}{C_{g,\lim}}>0.5\end{array}\right\}\cdots\cdots(15)$$

Analytical results show good coincidence with the experiments in Fig.7 and Fig.8. The sensitivity of the taper angle, which is associated with the model of the compatibility equation used to specify the shear strain intensity concerning the dimension and shape of pipes, is well predicted. The sensitivity of gravel and sand volumes in the mixture to the pressure needed is also similar to reality.

For computation of the pressure loss caused by the tapered unit, the same axial stiffness of aggregates as denoted in Eq. (12) and Eq.(13) for bent pipe units were utilized to adjust the analytical results to fit reality, we changed both the model of axial aggregate stiffness and the lateral stress ratio for a particular pipe unit.

This infinite combination of two models may happen to us owing to the stress and strain fields being degenerated from 3 to 1 dimension. This means that the set of axial stiffness and the lateral stress ratio is to be regarded as the constitutive model of aggregates as a whole. Within the work of 1-dimensional flow analysis, the axial stiffness is intentionally defined as a common model representing the intensity of particle stress transfer in the main flow, and the lateral stress ratio is regarded as a model representing a different mode of deformation.

(2) Sensitivity of paste phase model to deformability

The computation in the previous chapter is related only to the same water-to-cement ratio. Since the velocities of cement powder and water are assumed to be common in the computation, a change in cement and water mixture gives rise to different properties of the cement paste. In the above analysis, typical valuse for paste-wall friction were used as the paste model in Eq.(14). Since the axial contact stresses between the powder and water phases are treated as the hydrodynamic pressure which is not associated with the constitutive law but with the incompressibility and the requirement of compatibility[3], the paste stiffness model as the constitutive law does not explicitly appear in the framework of multi-phase modeling. In this study, the effect of cement paste on the drag force at segregation in Eq.(11) is less important too.

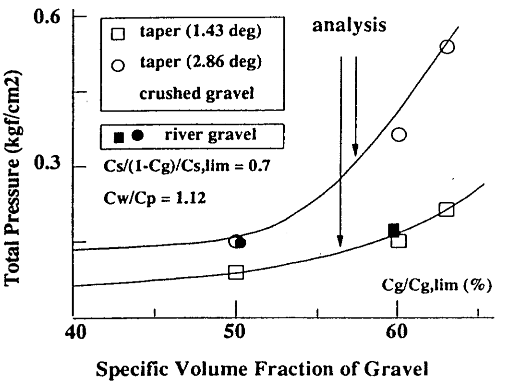

Fig.7 Total pressure at the inlet of tapered pipe with respect to the mixture content of gravel.

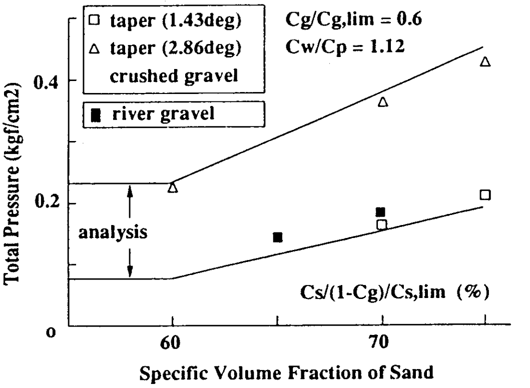

Fig.8 Total pressure at the inlet of tapered pipe with respect to the mixture content of sand.

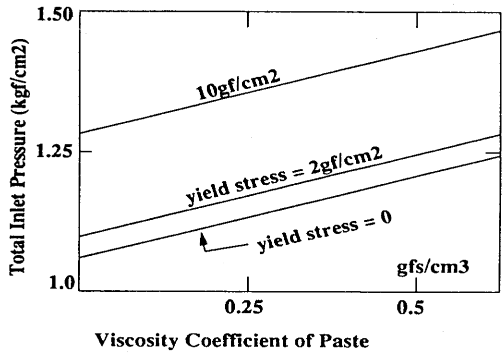

Fig.9 Sensitivity of viscosity coefficient and yield stress as the paste to the total pressure at the inlet of tapered pipe (2.86 deg). : $C_g/C_{g,\lim}=0.6$, $C_s/(1-C_g)/C_{s,\lim}=0.7$, rate of flow=10 cm/s

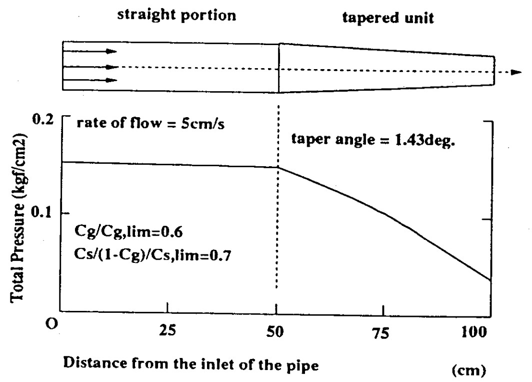

Fig.10 Distribution of the computed axial total pressure along the tapered pipe.

The sensitivity of the paste friction model in Eq.(10) to the computed pressure is shown in Fig.9 for the aggregate model in the previous chapter. The viscosity coefficient and yield stress in the cement paste phase in Eq.(10) are around 0.01-0.2 gf.s/cm² a nd 1-10 gf/cm² including the standard values in Eq. (14) when the water to cement ratio by weight changes by 0.3-0.7 without a chemical admixture agent[9]. Accordingly, the paste phase model on friction plays a minor role in the pressure drop at the deformed pipe provided that segregation can be avoided.

As shown in Fig.10, the pressure drop is negligibly small in a straight pipe where the paste friction is the primary source of pressure gradient. This means that the main factor affecting presssure in a defromed pipe is aggregate contact within the range of mix proportions given in Table 1. This conclusion holds so far as the straight pipe is not long enough to cause a substantial total pressure loss.

However, the experimental reality is that the mixture in terms of paste has a great influence on the pressure loss caused by deformed pipe units[6]. It is impossible to analytically explain the mechanism of paste sensitivity to pumpability using only the friction model of paste with the pipe wall. The chief source of deformability at the deformed pipes is the particle interaction model described by Eq. (9) . It may be reasonable to consider that the mixture of powder and water has an influence on particle interactions.

(3) Interaction of cement paste and aggregates

Microscopically speaking, the stiffness on contact stress represents the frequency of collisional events and the effectiveness of stress transfer per event concerned. Since the cement and water (paste) will change the frictional coefficient of contact of aggregates as coarser components, it is reasonable to assume that the aggregate stiffness model will be affected by the water-to-cement ratio of the paste between aggregates.

As shown in Fig.11, a lower water-to-cement ratio gives rise to greater contact friction between solids due to the presence of denser powders which enables higher contact force[11]. In analysis, the interaction between aggregates and cement powder and water is taken into account in terms of the partial stress.

This term represents the effect of stress gradient of finer components on the kinematics of coarser ones, such as buoyancy in the case of hydrostatics. Here, the contact stress of coarser components is assumed not to be affected by the presence of finer particles. Then, the change in friction has to be considered in the model of contact stress.

Table 1 Experimental Verification

Test Name	$\frac{C_g}{C_{g,\lim}}$ (%)	$\frac{C_s}{(1-C_g)C_{s,\lim}}$ (%)	$\frac{C_w}{C_p}$ (%)	Powder	Adm. (%)	Slump (cm)	Flow (cm)	Air (%)	Temp. °C	P.exp (kgf/cm^2)	Speed (cm/s)	Type of pipe	P.cal (kgf/cm^2)
CMIX5	46c	68	126	C	1	25	47x44	0.7	20	0.434	5.56	T2.86	0.600
29MIX6	56r	70	89	CSF	.95	22	36x39	1.5	21	1.15	4.80	T2.86	1.117
29MIX8	49r	69	88	CSF	.95	26	59x62	2.1	20	0.547	5.26	T2.86	0.623
30MIX3	51r	73	109	CSF	1.1	24	42x43	2.2	20	0.743	5.26	T2.86	0.660
30MIX9	53c	78	95	CSF	.95	24	43x43	1.3	19	0.791	5.00	T2.86	0.967
30MIX7	54c	70	89	CSF	.95	25	57x57	1.5	19	0.768	5.00	T2.86	0.874
30MIX8	54c	63	84	CSF	.95	26	60x59	1.1	19	0.761	5.20	T2.86	1.047
BT1	50r	70	112	C	1.0	24	38x38	2.5	16	1.569	4.00	B	1.535
TP2	50r	70	112	C	1.0	25	53x54	2.5	16	1.300	4.00	T1.43	1.350
19TP	50r	70	142	C	1.0	-	60x60	1.8	14	0.122	5.25	T1.43	0.170
19BB	50r	70	142	C	1.0	-	60x60	1.8	14	0.157	5.00	B	0.210
22TP2	50r	70	122	C	1.0	-	54x54	3.1	13	0.279	5.00	T1.43	0.230
22BB2	50r	70	122	C	1.0	-	54x54	3.1	13	0.591	4.76	B	0.320
25TP	50r	70	100	C	1.0	4	-	1.5	14	1.017	3.85	T1.43	1.050
25BB	50r	70	100	C	1.0	4	-	1.5	14	1.175	4.00	B	1.260
26TP	60r	70	142	C	1.0	19	40x40	2.3	11	0.708	4.00	T1.43	0.716
26BB	60r	70	142	C	1.0	19	40x40	2.3	11	0.695	3.85	B	0.698
26TP2	60r	70	122	C	1.0	20	37x37	2.4	13	0.545	4.55	T1.43	0.580
26BB2	60r	70	122	C	1.0	20	37x37	2.4	13	0.790	4.35	B	0.750
BB1	40r	70	112	C	1.0	-	59x59	1.9	27	0.532	5.56	B	0.422
BB2	50r	70	112	C	1.0	22	40x40	1.5	28	0.594	5.26	B	0.558
TPB2	50r	70	112	C	1.0	22	40x40	1.5	28	0.722	5.00	T2.86	0.744
BB3	60r	70	112	C	1.0	18	30x30	1.0	28	0.732	5.00	B	0.716
BB5	65r	70	112	C	1.0	3	-	1.0	29	0.854	3.85	B	0.921
BB6	60r	60	112	C	1.0	-	62x62	1.0	28	0.519	5.56	B	0.425
BB9	60r	70	112	C	1.0	18	29x29	1.3	26	0.655	5.00	B	0.716
TBB9	60r	70	112	C	1.0	18	29x29	1.3	26	0.773	5.00	T1.43	0.710
TBB10	65r	70	112	C	1.0	5	-	2.7	27	0.951	4.35	T1.43	1.130
TBB11	60r	65	112	C	1.0	-	22x22	1.0	23	0.636	5.00	T1.43	0.550
BB11	60r	65	112	C	1.0	-	22x22	1.0	23	1.022	5.00	B	1.022
TP	60c	70	112	C	1.0	13	-	2.5	22	0.717	5.00	T1.43	0.710
TP3	60c	70	112	C	1.0	13	-	2.5	22	1.665	4.55	T2.86	1.767
TP4	60c	75	112	C	1.0	16	-	2.2	21	0.970	5.00	T1.43	0.890
TP5	60c	75	112	C	1.0	16	-	2.2	21	2.000	4.00	T2.86	2.000
TPF1	60c	60	112	C	1.0	21	-	1.2	21	1.049	5.00	T2.86	1.070
TPF3	60c	60	112	C	1.0	21	-	1.2	21	0.922	4.00	T2.86	0.853
TPS1	50c	70	112	C	1.0	-	64x64	2.9	23	0.390	5.56	T1.43	0.330
TPL1	50c	70	112	C	1.0	-	64x64	2.9	23	0.768	5.00	T2.86	0.744
TPS2	50c	80	112	C	1.0	11	22x22	2.0	23	0.778	5.38	T1.43	0.628
TPL2	50c	80	112	C	1.0	11	22x22	2.0	23	1.790	5.38	T2.86	1.801
TPS8	63c	70	112	C	1.0	19	29x29	1.9	20	0.982	5.00	T1.43	0.977
TPL8	63c	70	112	C	1.0	19	29x29	1.9	20	2.450	4.59	T2.86	2.500

1) Gravel content : c = crushed gravel, r = river gravel.
2) Powder : C - ordinary Portland cement, CSF - cement(30%) + slag(30%) having Blaine value = $3000 cm^2/g$ + fly ash(40%) by weight.
3) Super-plasticizer : dosage specified by the percentage of the weight of powder.
4) Pressure abbreviated by P.exp and P.cal : measured and computed oil pressure in the pump cylinder. The friction between piston and pipe wall and the resistance at the straight portion of the device are deduced. The total pressure applied to concrete is 0.215 times the oil pressure (See Fig.2).
5) BT1 & TP2 : conducted 1 hour after placing concrete in the pump device.
6) Properties of crushed gravel : $C_{g,\lim} = 61.7\%$, $\rho_g = 2.63 g/cm^3$, FM = 6.51.
7) Properties of river gravel : $C_{g,\lim} = 64.3\%$, $\rho_g = 2.62 g/cm^3$, FM = 6.51.
8) Properties of sand : $C_{s,\lim} = 69.0\%$, $\rho_s = 2.53 g/cm^3$, FM = 2.94.

As far as the frictional behavior of cement is concerned, similar characteristics can be seen in Fig.12 and Fig.13, where the sensitivity of water-to-cement ratio to the total pressure needed is shown[6]. The aggregates were involved with exactly the same amount. Within the lower water-to-cement ratio range, the authors assumed the frictional contact modification factor (associated with Zone B in Fig.11) for the contact stiffness of aggregates by Eq.(12) and Eq.(13) corresponding to Cw/Cp=1.12 as follows.

$$\gamma_w=\frac{0.45}{C_w/C_p}\exp\left(\frac{0.2}{C_w/C_p-0.9}\right)\cdots\cdots\cdots\cdots\cdots(16)$$

where, γ_w is equal to unity when Cw/Cp=1.12, and is empirically specified become larger than unity when the water-to-cement ratio by volume is less than 112% as the control value so that we can take into account the higher frictional stress transfer among aggregates through the cement paste having lower water-to-cement ratio (See Zone B in Fig.11).

On the contrary, the mechanism of increasing friction is seen in Fig.11 (Zone A) when a larger water-to-cement ratio is assumed in turn. Similar behavior can be observed in Fig.12 and Fig.13 for the compact mixture of gravel as 60% of the specific volume fraction. It can be considered that water and cement powder serve as a coating agent which reduces the local roughness of aggregates at the same time. According to Fig.11, the following modification factor was introduced to model how firmly the paste coating is maintained during contact between gravel particles.

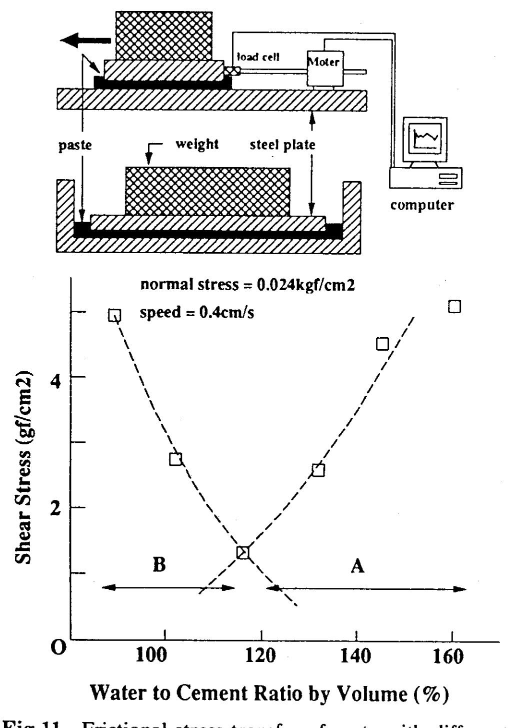

Fig.11 Frictional stress transfer of paste with different water to cement ratio[11].

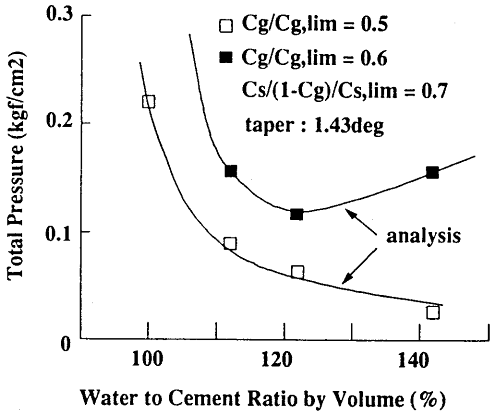

Fig.12 Calculated total pressure at the inlet of the tapered pipe with respect to the water to cement ratio.

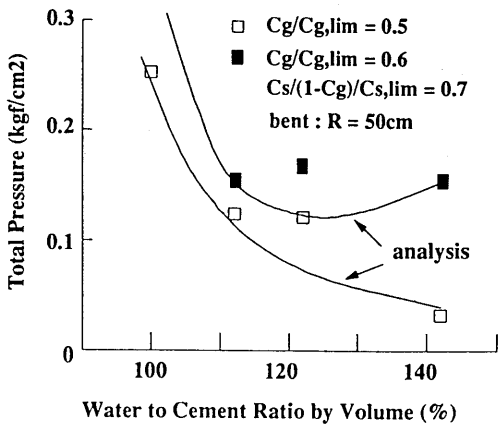

Fig.13 Calculated total pressure at the inlet of the bent pipe with respect to the water to cement ratio.

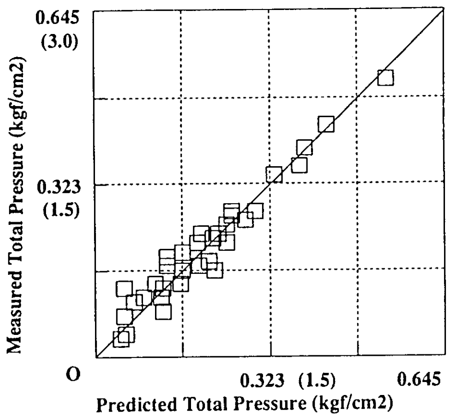

Fig.14 Comparison of measured and calculated total inlet pressure (pump oil pressure).

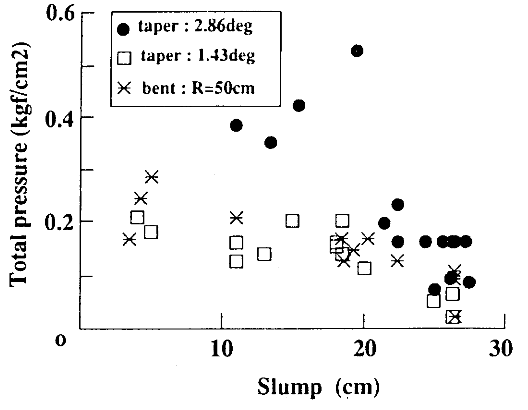

Fig.15 Relation between slump and the pressure needed to produce the stable flow of concrete.

$$\gamma_v=\left(\frac{10\cdot C_g}{C_{g,\lim}}-5\right)\left(\exp\left\{5\left(\frac{C_w}{C_p}-1.12\right)\right\}-1\right)+1\geq 1 \quad \cdots\cdots (17)$$

where, γ_v is equal to unity when Cw/Cp=1.12 and is empirically specified to become larger than unity when the water-to-cement ratio by volume is greater than 1.12 as the control value so that we can take into account the increasing friction among aggregates through the cement paste having larger water to cement ratio (See Zone A in Fig.11).

In Eq.(17), the specific volume fraction of gravel is included as a parameter since the smaller separation between gravel particles is thought to reduce the cohesive stability of paste around the aggregates[14]. This can be also observed in Fig.12 and Fig.13. Through a trial-and-error procedure, the authors finally propose the following empirical contact stiffness models which incorporate the volume fractions of aggregates and nonlinear frictional aspects of ordinary cement paste existing in the voids of aggregates:

$$K_g=\gamma_w\cdot\gamma_v\cdot K_g|_{\frac{C_w}{C_p}=1.12} \quad \cdots\cdots (18)$$

$$K_s=\gamma_w\cdot K_s|_{\frac{C_w}{C_p}=1.12} \quad \cdots\cdots (19)$$

It is thought that according to varying water-to-cement ratio, the lateral stress ratio would also change. Although no experimental data proving such a varying lateral stress ratio is available, it is reasonable to assume that the lateral stress ratio is associated with axial stiffness of contact, because both models are physically rooted in particulate contact between aggregates under deformation. Here, let us define the fictitious volume fraction of gravel as $Cg_{.eq}$ which is equivalent to Cw/Cp=1.12 as standard. In fact, this fictitious volume fraction can be mathematically obtained by solving Eq.(20).

$$K_g|_{\frac{C_w}{C_p}=1.12}\left(\frac{C_{g,eq}}{C_{g,\lim}}\right)=K_g\left(\frac{C_g}{C_{g,\lim}}\right) \quad \cdots\cdots (20)$$

As the lateral stress ratio given by Eq.(15) is applicable to the standard case Cw/Cp=1.12, the authors computed the lateral stress ratio by replacing Cg with $Cg_{.eq}$. This method implies that a unique relation exits between the lateral stress ratio of gravel and axial stiffness, and that the effect of water-to-cement ratio on both models is equable. Shown in Fig.12 and Fig.13 for tapered and bent pipes is the sensitivity of the water-to-cement ratio to total pressure generated by the flow through the deformed pipes. The analytical model has reasonable coincidence with the experiments.

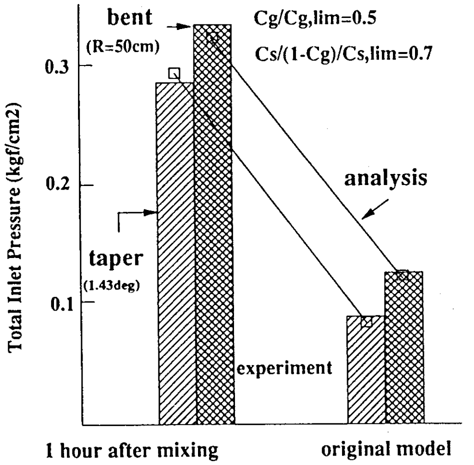

Fig.16 Elevated pressure by keeping fresh concrete asleep one hour after mixing.

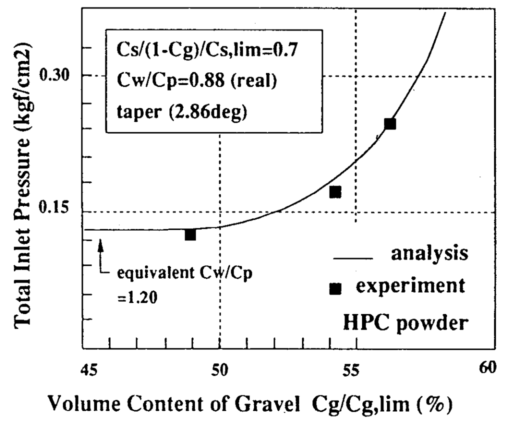

Fig.17 Predicted total inlet pressure for High Performance Concrete mix proportion.

(4) Experimental verification

Since the above stiffness and factors were defined to ensure that the computation is equivarent to the data for particular cases, other mixtures and their combination with the deformed pipes must be verified. Table 1 includes the analytical results and experiments of 42 cases[6] with concrete mixtures ranging for 45-60% as regards specific volume fraction of gravel, 63-80% for the specific volume fraction of sand, 84-142% for water-to-cement ratio by volume, and two types of tapered pipes and one sort of bent pipe. As for powder, ordinary Portland cement and mixed cementitious powder as used in self-compactable high-performance concrete[2] were adopted.

Fig.14 shows the correlation between computed and experimental results. Compared with the correlation between the value of slump and pressure (see Fig.15), the computational model is successful. This means that the consistency indicated by the slump test under gravity is not appropriate for judging the pumpability due to the different boundary conditions and external forces.

Table 1 also gives the calculated pump oil pressure using the proposed model. The total sectional averaged pressure at the inlet is 0.215 times the oil pressure according to the difference in cross-sectional area between the piston and the cylinder as shown in Fig.2. The coefficient of variation of the calculated-to-computed pressure ratio is 3.52% and the mean value is close to unity (1.012).

It must be pointed out that the material model for the effect of cement paste is forceful just under some particular production procedure. The well-known time-dependent deformability of fresh concrete is not explicitly formulated. The coagulation of powders suspended in water causes fresh concrete to stiffen[12], and in reality, the pumpability is proved to be much affected by the time-dependent stiffening, as shown in Fig.16, where one hour after mixing approximately three times greater pressure is needed at the inlet of the tapered and bent pipes.

If coagulation could be converted to the loss of freely movable water, the elevated pressure has to be computed with some equivalent water to cement ratio, because the loss of the effective free water is to be represented in terms of the water-to-cement ratio. In computation, the authors took up 99% of the equivalent water to cement ratio by volume as the alternate of original water to cement ratio (112%) by mixture. As shown in Fig.16, for both tapered and bent pipes, analytical results with the equivalent water-to-cement ratio seem successful. In future, we will aim at enhancement of the stress transfer model regarding cement powder and water in concrete.

Moreover, it should be understood that the proposed model can serve only when ordinary Portland cement is utilized. As reported by the authors[2,6], the kind of powder can change the features of stress transfer through particulate friction and collisions. Let us consider a mixed cementitious powder composed of ordinary cement, fly ash, and slag powders. Owing to the spherical shape of the fly ash and the wide-ranging grading of the powder phase, internal stress transfer will be reduced in comparison with the single ordinary Portland cement (see Table 1). This appears similar to the case of time-dependent hardening of fresh concrete.

Fig.17 shows the deformational resistance of concrete with mixed powders, what was innovated for the special purpose of a self-compactable concrete with high durability during transient and hardened stages. It is named self-compactable high-performance concrete[2]. The analytical results as shown in Fig.17 derived from a equivalent water-to-cement ratio of 112% based on ordinary cement as an alternate to the real water-to-powder ratio (88-89% by volume) with three mixed powders. As a matter of fact, normal cement concrete with $Cw/Cp=88\%$ will be definitely blocked to high resistance to deformation.

As discussed above, it is clear that models of powder suspensions in concrete mixtures are crucial to the versatility of the predictive method, especially in recent specifications of fresh concrete with a larger amount of powder. The time-dependency of powder suspension and coagulation and the type of powder have to be generalized in future, if we really seek a practical usage of the theory. Within the investigation reported in this paper, the aggregate model can be assumed to remain unchanged regardless of time and powder type.

4.CONCLUSION

In conclusion, the authors have to state clearly that the models proposed in this study are tentative despite the good coincidence of analysis with reality. The amount of super-plasticizer, the type of powder, the method of producing concrete and the interval before testing were all fixed, and not generally formulated. These factors invariably affect the fluidity and deformational resistance as well as pumpability. Although the role of paste will be investigated in future, the following conclusions can be reached:

(1) The partial stress concept in line with multi-phase modeling was verified to be a powerful tool for expanding the applicability of the model to a variety of concrete mix proportions.

(2) The stiffness, indicating the particle interactions of gravel and sand, was found to be different from each other, and influenced by the cement paste. The cement paste may play two roles in fresh concrete, e.g., as the matrix suspending the aggregates and as the agent of frictional stress transfer between coarser aggregates. The water-to-cement ratio changes the frictional coefficent between solids as well as the stiffness of the matrix itself. These aspects were considered in the stiffness model for the contact stresses of aggregates.

(3) The computation was examined by checking various mix proportions, boundary conditions, and rates of flow. In spite of the low correlation between pump pressure and slump value, computed pressure as one indicator of pumpability was shown to be successful.

The authors attempted a computational approach to the flow of fresh concrete having the features of both solid and liquid. As discussed previously, the model came close to some particular features of fresh concrete, but is still somewhat far from the reality at present. No matter how complete the model is, this multi-phase approach may serve as some sort of computerized test of concrete flow and placing without any external vibrations in line with the development of self-compactable concrete. Segregation under flow was proved to be an influential factor as regards overall workability and pumpability[3]. The computation exhibited powerful capabilities as one step on the way to the development owing to the multi-phase concept which enables us to deal with a variety of mixt proportions and segregation under flow.

ACKNOWLEDGMENTS

The authors are grateful to Prof.H. Okamura of the University of Tokyo for his suggestions and advice. This study was financially supported by Grant-in-Aid for Scientific Research No.8795443 from the Ministry of Education. The second author extends his gratitude to the Japanese Government for the allocation of a Monbu-sho scholarship to him during his academic stay at the University of Tokyo. The last author appreciates the financial support given by JICA to conduct analysis at Asian Institute of Technology.

References

[1] Okamura,H. : Waiting for innovation in concrete materials, Cement and Concrete, No.475, pp.2~5, Sept.1986 (in Japanese).
[2] Ozawa,K., Maekawa,K. and Okamura,H. : Development of high performance concrete, Journal of The Faculty of Engineering, The University of Tokyo(B), Vol.XLI, No.3, 1992.
[3] Maekawa,K., Ozawa,K. and Nanayakkara,A.S.M. : Multi-phase model for flow of liquid-solid assembly through pipelines, Proc.of JSCE, No.466/V-19, May, 1993.
[4] Nanayakkara,A.S.M., Ozawa,K. and Maekawa,K. : Deformational compatibility of aggregate phase for tapering flow of dense liquid-solid material, Proc.of JSCE, No.420/V-13, Aug., 1990.
[5] Nanayakkara,A.S.M., Ozawa,K. and Maekawa,K. : Deformational compatibility for solid phase of dense liquid-solid flow in bend pipes, Proc.of JSCE, No.426/V-14, Feb., 1991.
[6] Nanayakkara,A.S.M., Ozawa,K. and Maekawa,K. : Deformational resistnace of fresh concrete through bent and tapered pipes, Proc.of JSCE, No.466/V-19, May, 1993.
[7] Ozawa,K., Nanayakkara,A.S.M. and Maekawa,K. : Evaluation of aggregate particle motion in liquid-solid flows of model concrete, Proc.of JSCE, No.408/V-11, Aug., 1989.
[8] Ede, A.D. : The resistance concrete pumped through pipelines, Magazine of Concrete Research, Nov., 1957
[9] Tanigawa,Y., Mori,H., Tsutusui,K. and Kurokawa,Y. : Constitutive law and yield criterion of fresh concrete, Proc. of JCI, Vol.9, No.1, 1987 (in Japanese).
[10] Tangtermsirikul, S. and Maekawa,K. : Deformational model for solid phase in fresh concrete under compression, Proc. of JCI, Vol.11, 1989.
[11] Izumi,T., Maekawa,K., Ozawa,K. and Kunishima,M. : Influence of paste on the frictional resistance between solids, Proc. of JCI, Vol.10, No.2, 1988 (in Japanese).
[12] Hattori,K. and Izumi,K. : A new viscosity equation for non-Newtonian suspensions and its application, Rheology of fresh cement and concrete, E.&F.N.Spon, 1991.
[13] Kishitani,T., Sugawara,T., Oka,S. and Sata,K. : Flowability of fresh cementpaste and mortar : Method of measurement, Proc. of AIJ, Sept., 1980 (in